Exploiting Perceptual Anchoring for Color Image Enhancement

Kuang-Tsu Shih and Homer H. Chen, *Fellow, IEEE*

***Abstract*—The preservation of image quality under various display conditions becomes more and more important in the multimedia era. A considerable amount of effort has been devoted to compensating the quality degradation caused by dim LCD backlight for mobile devices and desktop monitors. However, most previous enhancement methods for backlight-scaled images only consider the luminance component and overlook the impact of color appearance on image quality. In this paper, we propose a fast and elegant method that exploits the anchoring property of human visual system to preserve the color appearance of backlight-scaled images as much as possible. Our approach is distinguished from previous ones in many aspects. First, it has a sound theoretical basis. Second, it takes the luminance and chrominance components into account in an integral manner. Third, it has low complexity and can process 720p high-definition videos at 35 frames per second without flicker. The superior performance of the proposed method is verified through psychophysical tests.**

***Index Terms*—Anchoring theory, color appearance model, color image enhancement, human perception.**

I. Introduction

MOST multimedia devices are equipped with a panel display today [1], [2]. This is unlikely to change in the foreseeable future. The panel display usually consumes a significant portion of the energy of a multimedia device. For example, among all components, the backlight module of a liquid crystal display (LCD) may consume as much as 50% of the total power for a smartphone in the video playing mode [3]. This is a major concern for most mobile devices because of limited battery capacity. Reducing the power of the backlight module is an effective means to save energy and extend the battery life. However, dim backlight severely degrades the quality of image luminance and chrominance. As shown in Fig. 1(a), when the backlight is switched to a low power level, the color and detail of the woods region in the image can hardly be seen. To further illustrate the chrominance degradation, two patches illuminated with various backlight intensities are shown in Fig. 1(b), where the pink block and the achromatic gray block are set at the same luminance level. We can see that the two patches become less distinguishable as the backlight goes dimmer.

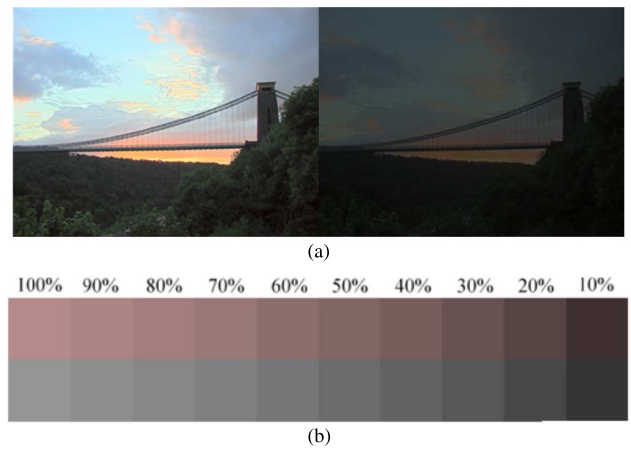

Fig. 1. Demonstration of the effect of backlight-scaling on image appearance. All backlight-scaled images in this figure are generated by the procedure described in Section V-B. (a) The original image (left) and its backlight-scaled image (right). (b) Color patches illuminated with backlight of different intensities. The backlight-scaling ratios are shown at the top of each column.

The importance of the need for compensating the undesirable effect of dim backlight cannot be overstated for mobile devices nowadays [4], [5]. The issue can be broadly described as that of color image enhancement across different reproduction conditions, whether the backlight-scaled image is displayed on the same LCD or not. The issue exists in many other multimedia applications as well. For example, in high dynamic range (HDR) image tone mapping, the luminance of a scene spanning nearly ten orders has to be reproduced on a display with merely three orders of dynamic range [6]. Another example is ubiquitous projection, where a projector has to overcome the effects of color and texture of a non-white projection surface so that the image would appear as if it were projected on a white screen [7], [8]. Likewise, in energy-aware video streaming where the multimedia clients often work in a low-backlight condition to save energy, the server has to take the effect of dim backlight on the display into consideration to achieve high quality of experience on the client side [9], [10].

The image is ultimately watched by a human. Therefore, properties of the human visual system (HVS) have to be taken into consideration for image enhancement. Because color perception is a psychological process, preserving color sensation across different image reproduction conditions is often more

Manuscript received April 22, 2015; revised September 08, 2015 and November 04, 2015; accepted November 18, 2015. Date of publication November 25, 2015; date of current version January 15, 2016. This work was supported in part by the National Science Council of Taiwan under Contract NSC 100-2221-E-002-197-MY3, in part by the National Taiwan University under Contract NTU-CESRP-102R7609-2, and in part by Himax Technologies, Inc. under Contract 101-S-C37. The associate editor coordinating the review of this manuscript and approving it for publication was Dr. Wolfgang Hurst.

K.-T. Shih is with the Graduate Institute of Communication Engineering, National Taiwan University, Taipei 10617, Taiwan (e-mail: shihkt@gmail.com).

H. H. Chen is with the Department of Electrical Engineering, Graduate Institute of Communication Engineering and the Graduate Institute of Networking and Multimedia, National Taiwan University, Taipei 10617, Taiwan (e-mail: homer@ntu.edu.tw).

Color versions of one or more of the figures in this paper are available online at http://ieeexplore.ieee.org.

Digital Object Identifier 10.1109/TMM.2015.2503918

important than retaining the physical color. This is especially the case for the enhancement of backlight-scaled images considered in this work, for which the image luminance cannot be recovered unless the backlight power is returned to the full level.

Most previous methods for backlight-scaled image enhancement [11]–[14] either overlook the impact of color appearance on image quality or separately consider the processing of luminance and chrominance, leading to improper or mismatched chrominance adjustment.

The study of HVS suggests that our brain processes a color stimulus relative to an anchor (a reference value) corresponding to the display condition [15]. Our color sensation of a stimulus is maintained under a different display condition if the stimulus relative to the anchor is preserved. In this paper, this property of human visual perception is exploited for backlight-scaled image enhancement. Our approach allows the compensation of the undesired effects of dim backlight in an integral manner. It has a sound theoretical basis—the anchoring property of HVS—and enhances the color appearance of images in a way that matches human perception. Furthermore, it works consistently well for different images and avoids unnatural color appearance caused by the mismatch between luminance and chrominance components. The low computational complexity of this approach is attractive for energy-aware multimedia applications [16]–[19].

This paper distinguishes from its conference version [20] in three aspects. First, a post gamut mapping algorithm is developed to better preserve the image details. Second, new experiments are conducted to compare the proposed method with existing methods. Lastly, a discussion on the impact of the color appearance model on the overall system performance is provided.

II. Related Work

In this section, we give an overview of perceptual models for human color perception and methods for enhancing image appearance.

A. Color Appearance Models

To accurately preserve the color sensation across various display conditions, a precise quantification of color appearance that matches human perception is required. This subject has been studied for long in color science. Many color models with emphasis on the effect of viewing condition have been developed recently.

An early model called XYZ quantifies color sensation through a strictly controlled matching experiment [21]. It has two disadvantages. First, it is not perceptually uniform. In other words, the Euclidean distance between two points in the XYZ space does not correlate well with the perceptual difference between the color stimuli represented by the points. Second, it works only if the viewing condition in the original experiment is satisfied.

To improve perceptual uniformity, color opponent spaces such as CIELAB [22] were developed. Unlike the XYZ model, the three dimensions of a color opponent space have clear perceptual meaning: One represents lightness, one the red-green opponent color channel, and the other the yellow-blue opponent color channel. Although such spaces have been proven to be more perceptually uniform than the XYZ model, the viewing condition is not taken into account.

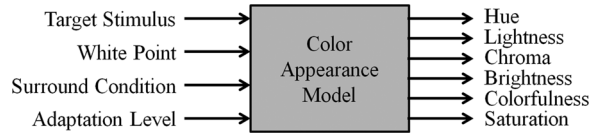

Fig. 2. Inputs and outputs of a typical color appearance model.

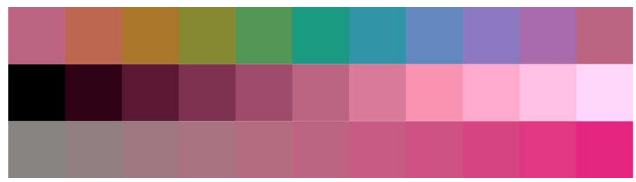

Fig. 3. Color patches having different hue values (top row), lightness values (middle row), and chroma values (bottom row). The value increases from left to right for lightness and chroma.

A color appearance model takes into account the effect of viewing condition on color perception [15] and hence is capable of modeling many color appearance phenomena that cannot be modeled by the XYZ space or the color opponent spaces. The typical inputs and outputs of a color appearance model are shown in Fig. 2. The inputs include the XYZ values of the target color stimulus along with a set of parameters describing the viewing condition. The outputs are the predictors of the color appearance attributes: hue, lightness, brightness, chroma, colorfulness, and saturation. Fig. 3 shows color patches that differ in hue, lightness, and chroma. These attributes can be classified into two categories: absolute and relative. The difference between them is subtle but important (see Section III).

There are many color appearance models developed for various applications [22]–[26]. Among them, CIECAM02 [27] is recommended for general color reproduction due to its accuracy and simple reversibility [15].

B. Gamut Mapping

Gamut mapping is the operation of assigning a point in the target gamut to a corresponding point in the source gamut. It is usually incorporated in color reproduction systems [28], [29]. Existing gamut mapping algorithms (GMAs) can be classified into two categories: reduction and expansion. Reduction GMAs are designed for the scenario where the volume of the target gamut is smaller than that of the source gamut, whereas expansion GMAs are designed for the scenario where the volume of the target gamut is larger than that of the source gamut. Current research on gamut mapping falls mostly into the first category, so does this work because the target low-backlight gamut is much smaller than the source full-backlight gamut.

Reduction algorithms can be further categorized into two types according to their mapping strategy. One type adopts the clipping strategy [30] and only acts on the points outside the target gamut while leaving the other in-gamut point intact. In contrast, the other type adopts the compression strategy [31]–[34] and remaps every point in the source gamut no matter whether the point is in the target gamut or not. For this type of

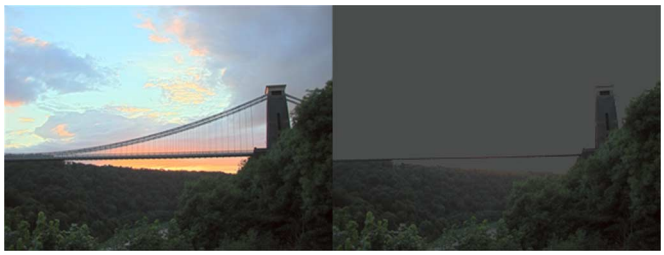

Fig. 4. GMA with the clipping strategy wipes out image details in bright regions. The left is the original image and the right is the gamut-mapped image.

GMAs, the color appearance attributes (i.e. lightness, chroma, and hue) can be compressed sequentially [31], [32] or simultaneously [33], [34]. For situations where the source and target gamuts have significantly different volumes or shapes, clipping may result in loss of details as shown in Fig. 4. On the other hand, when there are only a limited number of out-of-gamut pixels, compression is usually avoided because it introduces unnecessary distortion to the in-gamut pixels.

The performance of existing GMAs is highly dependent on the target application. That is, a GMA good for some source and target gamuts may fail others. Although a general-purpose GMA is desired, no satisfactory solution has been found yet. In addition, there is no consensus about the state-of-the-art GMA due to the lack of a good evaluation method [28].

C. Enhancement Methods for Backlight-Scaled Images

Existing enhancement methods for backlight-scaled images can be classified into two categories. One category aims at preserving the luminance of pixels across different power levels of the backlight [35], [36], whereas the other one targets enhancing the visibility of images illuminated with dim backlight [12]–[14].

To preserve the luminance of each pixel, methods in the first category determine the lowest possible dimming ratio (usually no lower than 50%) on the fly according to the image content. Targeting primarily at energy saving, these methods usually require the local intensity of the backlight to be controllable.

On the other hand, methods in the second category can be applied to images illuminated by backlight with a very low dimming ratio (as low as 10%). The typical procedure of such methods is shown in Fig. 5. The luminance layer is first extracted (either in HSV space [14] or YCbCr space [12], [13]) from the input image and then decomposed into a detail layer (high-passed) and a base layer (low-passed). Such decomposition is implemented through a convolution with a spatially invariant low-pass kernel [12], an adaptive nonlinear filtering scheme based on the just noticeable difference (JND) [13], or a minimization of the total variation of the base layer [14]. The two layers are then processed independently and combined with the chrominance layer of the input image to generate the enhanced result. Typically, the compression of luminance is performed only on the base layer to preserve local contrast as much as possible, while the detail layer is either untouched [12], [13] or passed to a contrast enhancement scheme [14]. In contrast to the delicate processing of the luminance layer, the chrominance layer is left untouched by most existing methods.

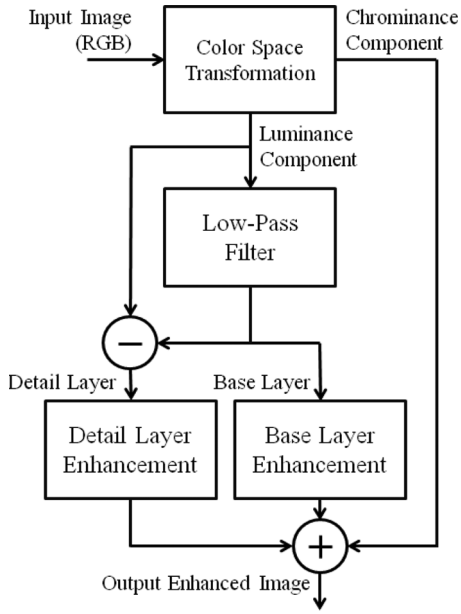

Fig. 5. Flowchart of conventional backlight-scaled image enhancement.

Fig. 6. Conventional backlight-scaled image enhancement algorithms fail to preserve the contrast between the woods and the sky. The left is the original image and the right is the result of Pei [10].

One main drawback of such methods is that the *global* contrast may not be preserved in the enhanced image. As shown in Fig. 6, the luminance contrast between the bright region (sky) and the dark region (woods) in the original image is destroyed in the enhanced image. In addition, such methods only work on the luminance layer and pay little attention to the chrominance degradation.

D. Display Characterization

Display characterization is important for accurate color reproduction. It aims at characterizing the relation between input RGB values and output XYZ values of displays. The relation is usually expressed by a mathematical function (the display model) with a set of parameters.

A typical procedure of display characterization goes as follows. First, a display model is determined for the target display. Note that, in this step, only the form of the mathematical model is determined and the parameters are not yet known. Next, a sample set containing multiple color samples is picked, and the XYZ values of the color samples are measured using a colorimeter. The number of color samples increases with the number of parameters of the display model. Finally, the obtained groundtruth XYZ values are used to estimate the parameters of

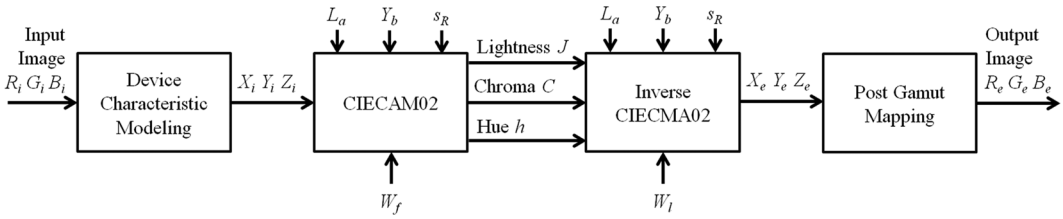

Fig. 7. Flowchart of the proposed algorithm. The white points for the forward and the inverse models are set different.

the display model by regression. After the parameters are obtained, the XYZ value of an arbitrary RGB input is predicted.

There are many display models available for characterizing various displays [37]. For example, the gain-offset-gamma (GOG) model [38] targets cathode ray tube (CRT) displays, and the S-curve model [39] and the polynomial model [40] are developed for LCDs.

III. The Anchoring Property

Anchoring is essential to human color perception and our work. For the same physical stimulus, the perceptual response becomes higher when the anchor is at a lower level. We discuss the anchoring property of HVS in this section.

It is widely accepted that HVS functions more than a light sensor. To illustrate this point, consider a piece of paper at night and a lamp under sunlight. Although physically the latter emits more light than the former, we still perceive the former to be brighter. This common experience suggests that HVS judges color appearance in a relative manner by comparing the physical color of a stimulus with the anchor determined by the viewing condition. Because the anchor at night is much darker than that in daytime, the paper is perceived brighter than the lamp. Similarly, for an LCD, when the backlight intensity is lowered, the HVS tends to overestimate the light emitted by the display, resulting in a higher perceptual response. The overestimation is, again, the result of a darker anchor corresponding to the low-backlight display.

This important property of the HVS has been incorporated into color appearance models. As described in Section II-A, a color appearance model generates both absolute and relative perceptual attributes. Relative attributes are used to describe visual sensations that involve a comparison with the anchor, whereas the absolute attributes are used to describe sensations that are independent of the anchor. Although in some situations (e.g. observing a light source in a dark room) the absolute attributes are more meaningful than the relative attributes, the relative perception often plays a more important role in our daily visual experiences.

IV. The Proposed Enhancement Algorithm

To cope with the anchoring property of human color perception, our enhancement algorithm preserves the relative attributes (lightness, hue, and chroma) across different backlight intensities. The flowchart of the proposed enhancement algorithm is shown in Fig. 7. It has three main steps, namely, display characterization, color reproduction, and post gamut mapping. We describe them in detail in this section.

A. Display Characterization

Since our enhancement algorithm targets faithful color reproduction, high-precision characterization is necessary. For that, we adopt the following display model:

$$\begin{bmatrix} X \\ Y \\ Z \end{bmatrix} = \mathbf{M} \begin{bmatrix} R_l \\ G_l \\ B_l \end{bmatrix} = \begin{bmatrix} m_{rx} & m_{gx} & m_{bx} \\ m_{ry} & m_{gy} & m_{by} \\ m_{rz} & m_{gz} & m_{bz} \end{bmatrix} \begin{bmatrix} R^{\gamma_r} \\ G^{\gamma_g} \\ B^{\gamma_b} \end{bmatrix} \quad (1)$$

where γ_r, γ_g, and γ_b, respectively, denote the gamma values of the red, green, and blue channels, (R, G, B) denotes the normalized device-dependent pixel value in the input image, (R_l, G_l, B_l) denotes the linear RGB value, and (X, Y, Z) denotes the resulting XYZ tristimulus value. (1) transfers the input pixel value from the device-dependent RGB space to the device-independent XYZ color space.

There are a total of 12 model parameters (three gamma values and nine transformation matrix entries) in (1) that need to be determined. Define the following sample values:

$$C_R = \left\{ \left(\frac{15+16k}{255}, 0, 0 \right) | k = 0, 1, 2, \cdots 15 \right\} \quad (2)$$

$$C_G = \left\{ \left(0, \frac{15+16k}{255}, 0 \right) | k = 0, 1, 2, \cdots 15 \right\} \quad (3)$$

$$C_B = \left\{ \left(0, 0, \frac{15+16k}{255} \right) | k = 0, 1, 2, \cdots 15 \right\} \quad (4)$$

and

$$C_A = \left\{ \left(\frac{15+16k}{255}, \frac{15+16k}{255}, \frac{15+16k}{255} \right) | k = 0, 1, 2, \cdots 15 \right\}. \quad (5)$$

C_R contains red samples, C_G green samples, C_B blue samples, and C_A achromatic samples. These samples (a total of 60) plus the RGB value $(0, 0, 0)$ form a sample color set. After the ground truth of the 61 sample colors in the XYZ space is obtained using a colorimeter, the 12 model parameters are estimated by convex optimization.

The characterization is performed for the full-backlight display and the low-backlight display. The resulting estimated gammas are denoted by $\gamma_{r,f}$, $\gamma_{g,f}$, and $\gamma_{b,f}$ for the full-backlight display and $\gamma_{r,l}$, $\gamma_{g,l}$, and $\gamma_{b,l}$ for the low-backlight display. Likewise, the resulting transformation matrices for the full-backlight and the low-backlight displays are denoted by $\mathbf{M}_f$ and $\mathbf{M}_l$, respectively. The parameter estimation does not need to be performed for each new image. The same parameters can be used till the display is recalibrated.

The XYZ tristimulus value (X_i, Y_i, Z_i) of an arbitrary pixel in the original image is obtained from the RGB value

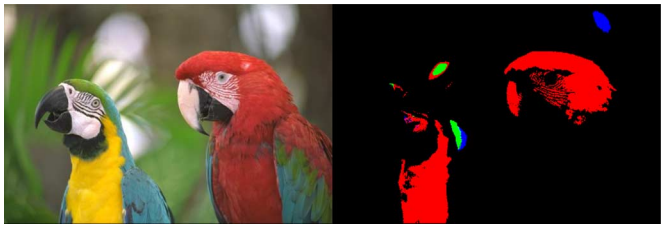

Fig. 8. Original image (left) and the out-of-gamut pixels (right), where pixels whose red channel is not in the [0 1] range are marked red. Similarly, the green and blue out-of-gamut pixels are marked in the right image.

(R_i, G_i, B_i) by substituting $(R, G, B) = (R_i, G_i, B_i)$, $\gamma_r = \gamma_{r,f}$, $\gamma_g = \gamma_{g,f}$, $\gamma_b = \gamma_{b,f}$, and $\mathbf{M} = \mathbf{M}_f$ into (1).

B. Color Reproduction

We seek to preserve the relative attributes of lightness, chroma, and hue using a color appearance model. Such appearance reproduction has been known since the early 1990s and is adopted in our algorithm. In this step, the point of the highest luminance in the display gamut is selected to be the anchor. This way, the anchor is only determined by the dimming ratio, which is independent of the input image. Among the existing color appearance models, we adopt CIECAM02 in this work for its accuracy and the simplicity of the inverse operation [41]. The entire set of equations in CIECAM02 can be found in [27]. For convenience, the input-output relationship of CIECAM02 is denoted by $\psi(\cdot)$. The inputs are the XYZ tristimulus value of the target, the luminance of the adaptation field, the luminance of the background field, and the surround condition. The outputs are the six attributes of color perception.

In this step, we first compute the XYZ value of the anchor for the full-backlight display W_f by setting $R = G = B = 1$, $(\gamma_r, \gamma_g, \gamma_b) = (\gamma_{r,f}, \gamma_{g,f}, \gamma_{b,f})$, and $\mathbf{M} = \mathbf{M}_f$ in (1). Similarly, we obtain the anchor for the low-backlight display W_l by setting $R = G = B = 1$, $(\gamma_r, \gamma_g, \gamma_b) = (\gamma_{r,l}, \gamma_{g,l}, \gamma_{b,l})$, and $\mathbf{M} = \mathbf{M}_l$ in (1). Next, we obtain the relative attributes (lightness J, chroma C, and hue h) from the color appearance model

$$(J, C, h) = \psi(X_i, Y_i, Z_i, W_f, L_a, Y_b, s_R) \tag{6}$$

where L_a is the absolute adapting luminance measured in $\mathrm{cd/m^2}$, Y_b is the relative luminance of the background, and s_R is the surround parameter. The enhanced XYZ value is obtained from the inverse color appearance model $\psi^{-1}(\cdot)$ by

$$(X_e, Y_e, Z_e) = \psi^{-1}(J, C, h, W_l, L_a, Y_b, s_R). \tag{7}$$

Note that the low-backlight anchor W_l serves as the white point in the inverse color appearance model.

C. Post Gamut Mapping

The enhanced XYZ value (X_e, Y_e, Z_e) may fall outside the low-backlight gamut for some pixels. A sample image of out-of-gamut pixels is shown in Fig. 8. We see that there are still a few bright and highly-saturated pixels that are outside the low-backlight gamut. These out-of-gamut pixels have to be brought back in the display gamut. To do this, we adopt a soft clipping GMA here to avoid introducing unnecessary distortion to the in-gamut pixels, which are the majority.

TABLE I
ESTIMATED DISPLAY PARAMETERS

Parameter*	Value	Parameter*	Value
$\gamma_{r,f}$	2.4767	$\gamma_{r,l}$	2.2212
$\gamma_{g,f}$	2.4286	$\gamma_{g,l}$	2.1044
$\gamma_{b,f}$	2.3792	$\gamma_{b,l}$	2.1835
$\mathbf{M}_f$	$\begin{bmatrix} 95.57 & 64.67 & 33.01 \\ 49.49 & 137.29 & 14.76 \\ 0.44 & 27.21 & 169.83 \end{bmatrix}$	$\mathbf{M}_l$	$\begin{bmatrix} 4.61 & 3.35 & 1.78 \\ 2.48 & 7.16 & 0.79 \\ 0.28 & 1.93 & 8.93 \end{bmatrix}$

*The symbols are defined in Section IV-A.

To alleviate the undesired loss of image details caused by clipping (discussed in Section VII-B), we adopt a weighted-average approach that outputs a linear combination of the clipped RGB value and the original RGB value for each pixel. Since both the clipped and the original RGB value are within the low-backlight gamut, their weighted average is guaranteed to be inside the gamut as well. Furthermore, through the selection of the weight, the output value of a pixel can be controlled towards the original pixel value or the clipped pixel value. Since brighter and more saturated colors suffer more from the clipping artifact, the weight for such pixels can be adjusted accordingly to preserve the image details.

In this step, a color transformation from the XYZ space to the RGB space is first applied to obtain the intermediate RGB value (R', G', B') for each pixel

$$(R', G', B') = \left(R_{e,l}^{\frac{1}{\gamma_{r,l}}}, G_{e,l}^{\frac{1}{\gamma_{g,l}}}, B_{e,l}^{\frac{1}{\gamma_{b,l}}} \right) \tag{8}$$

where

$$[R_{e,l}\ G_{e,l}\ B_{e,l}]^{\mathrm{T}} = \mathbf{M}_l^{-1}[X_e\ Y_e\ Z_e]^{\mathrm{T}}. \tag{9}$$

The clipped value (R_c, G_c, B_c) of a pixel is computed by

$$(R_c, G_c, B_c) = (f(R'), f(G'), f(B')) \tag{10}$$

where

$$f(x) = \begin{cases} x, & \text{if } 0 \le x \le 1 \\ 1, & \text{if } x > 1 \\ 0, & \text{if } x < 0. \end{cases} \tag{11}$$

Here, a pixel is out-of-gamut if its R', G', or B' is outside the range [0, 1]. The final enhanced RGB value (R_e, G_e, B_e) is obtained by linearly combining the clipped RGB value and the original RGB value

$$\begin{bmatrix} R_e \\ G_e \\ B_e \end{bmatrix} = (1 - JC) \begin{bmatrix} R_c \\ G_c \\ B_c \end{bmatrix} + JC \begin{bmatrix} R_i \\ G_i \\ B_i \end{bmatrix}. \tag{12}$$

We choose JC as the weight on (R_i, G_i, B_i) so that the enhanced RGB value of bright and saturated pixels are biased towards their original RGB value. Such bias reduces the loss of image details.

The proposed post gamut mapping algorithm has low computational complexity because it is performed in the RGB space (where the gamut is cube-shaped and hence the calculation of the gamut boundary is straightforward) instead of the XYZ

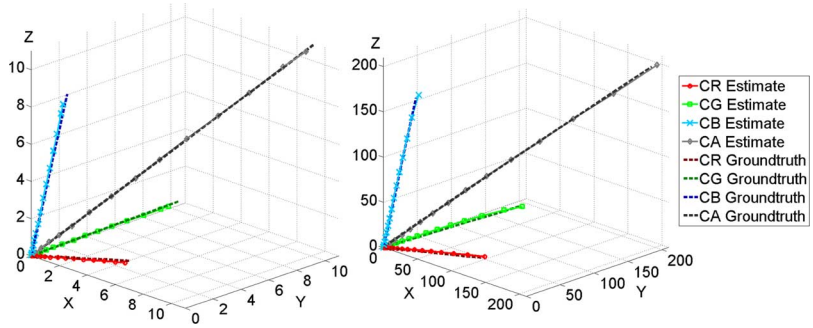

Fig. 9. The dashed-line curves connect the ground truth of the samples C_R, C_G, C_B, and C_A and the solid-line curves connect the estimated XYZ values of the samples. The left is the result for the low-backlight display and the right is the result for the full-backlight display.

space (where the gamut has non-planar boundary). In addition, parallel processing can be carried out to achieve further acceleration because of the spatial invariance property of the algorithm, where the computation involved in (8)–(12) for each pixel is independent of its neighbors.

V. Experimental Results

The success of the proposed algorithm is hinged on the performance of display characterization. Two experiments are set up to evaluate the accuracy of display characterization and the quality of the enhanced images.

A. Performance Evaluation of Display Characterization

This experiment involves three steps: color sample measurement, display parameter estimation, and calculation of estimation error. In the first step, a Laiko DT-101 colorimeter is used to measure the XYZ value of every sample in C_R, C_G, C_B, and C_A defined in (2)–(5). In the second step, the measured values are used to estimate the display parameters $(\gamma_r, \gamma_g, \gamma_b, \mathbf{M})$ according to the procedure described in Section IV-A. The estimated parameters are listed in Table I. In the third step, the estimation error is obtained by computing the average CIEDE2000 color difference between the ground truth and the estimated XYZ values. The average CIEDE difference is 2.60 for the full-backlight display and 2.65 for the low-backlight display.

The dashed curves in Fig. 9 connect the ground truth of the samples, and the solid curves connect the estimated XYZ values of the samples. We can see that the solid curves are in close proximity to their corresponding dashed curves in the XYZ space, indicating that the display model (1) and the estimated parameters together accurately characterize the displays.

B. Quality Evaluation of Enhanced Images

We apply the proposed algorithm to enhance uniform color patches and natural images illuminated with dim backlight in this experiment. The parameters of CIECAM02 are set as follows according to the viewing condition: The absolute luminance of the adapting field L_a is 63 (measured by a colorimeter), and the relative luminance of the background Y_b is 25 (one fourth of the relative luminance of the reference white). Since the experiments are performed in a well-illuminated lab, the surround condition is set to "average" according to Fairchild [15].

It should be pointed out that the results should be evaluated on an LCD rather than on a printout of the paper. Ideally, the performance evaluation should be conducted on a pair of displays having the same parameters shown in Table I. To make it convenient for the reader to evaluate the images in one display, simulated low-backlight images are shown here. These images are generated in such a way that, when illuminated with full backlight, they would appear identical to the enhanced images illuminated with dim backlight. Specifically, the RGB value (R_s, G_s, B_s) of the simulated image is computed as follows:

$$(R_s, G_s, B_s) = \left(R_{s,l}^{\frac{1}{\gamma_{r,f}}}, G_{s,l}^{\frac{1}{\gamma_{g,f}}}, B_{s,l}^{\frac{1}{\gamma_{b,f}}} \right) \tag{13}$$

where

$$\begin{bmatrix} R_{s,l} \\ G_{s,l} \\ B_{s,l} \end{bmatrix} = \mathbf{M}_f^{-1} \mathbf{M}_l \begin{bmatrix} R_e^{\gamma_{r,l}} \\ G_e^{\gamma_{g,l}} \\ B_e^{\gamma_{b,l}} \end{bmatrix}. \tag{14}$$

For a thorough quality evaluation using two displays, the enhanced images are available on our website.[1]

The experimental results for uniform color patches and natural images are shown in Figs. 10 and 11, respectively. For the ease of evaluation, we slightly increase the brightness of the resulting images. Specifically, these images are generated by (13) and (14) but with a different set of low-backlight display parameters obtained by characterizing the LCD with a higher backlight intensity. For the reader to have a feel of the actual brightness, we show in Fig. 12 one set of results that are generated with the original display parameters. The proposed method is compared against six existing methods: Pei [14], Huang [13], temporally aware backlight scaling (TABS) [11], adaptive backlight image enhancement (ABIE) [12], multi-scale retinex algorithm (Retinex) [9], and gamma correction (Gamma) with a fixed gamma value 0.5. In Fig. 10, uniform white patches are appended to indicate the backlight intensity.

From the results shown in Fig. 10, we can see that the color patches generated by the retinex algorithm, ABIE and TABS are too dark and do not resemble the original image, and that the chroma and hue of the gamma corrected results deviate seriously from the original patch. On the other hand, the lightness of the green patch in the first row produced by Pei is overly enhanced. This is more obvious if we compare the contrast between the green patch and the red patch in the second row before and after enhancement. Likewise, Huang tends to

[1]"MPAC Lab," [Online]. Available: https://goo.gl/RTzqLq

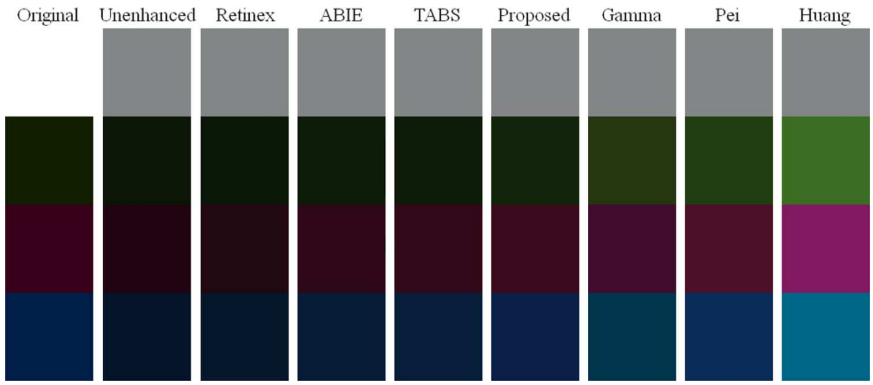

Fig. 10. Color enhancement performance comparison. The first column shows the original patches illuminated with full backlight, the second column shows the patches illuminated with dim backlight without enhancement, and the other columns show the enhanced patches produced by various methods.

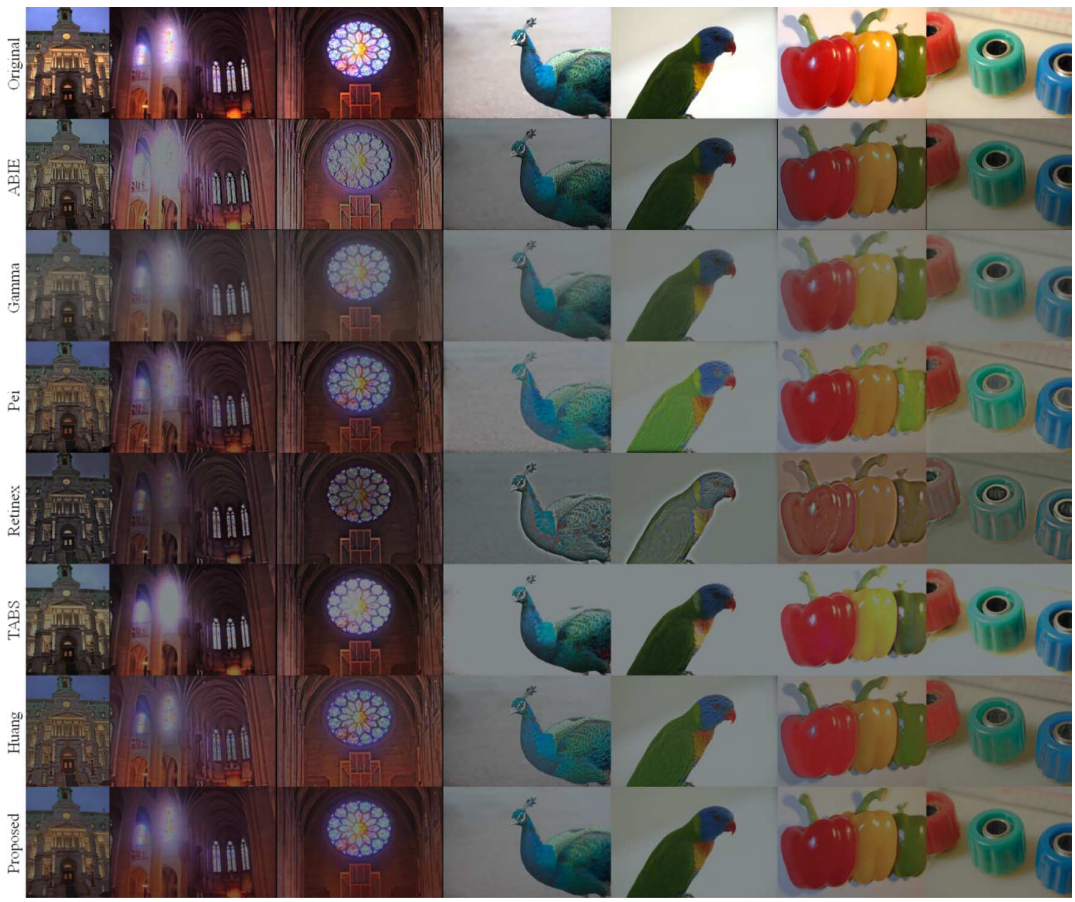

Fig. 11. Original images illuminated with full backlight and the enhanced images illuminated with dim backlight (simulated). Images in each row are generated by the same method, and the name of the method is shown on the left.

Fig. 12. Original image illuminated with full backlight and the enhanced images illuminated with dim backlight (simulated). The simulated backlight intensity is set equal to that of the real low-backlight display.

generate overly bright and saturated results. Because both Pei and Huang decompose an image based on the spatial frequency of the image, they may fail for uniform color patches, which have no high-frequency component.

From Fig. 11 we can see that ABIE and TABS fail to preserve details in the bright region of the image (e.g. the color glass windows, particularly the one with strong glare, in the second column and the third column), and that the chroma pro-

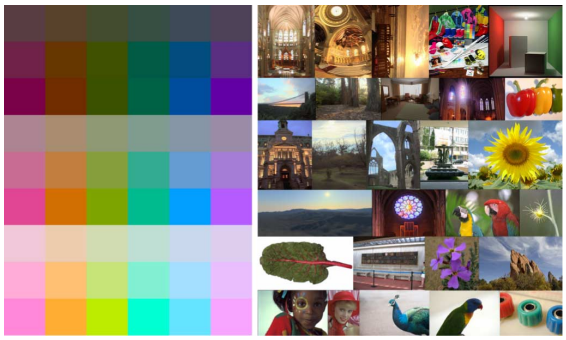

(a) (b)

Fig. 13. (a) shows the 54 color patches and (b) shows the 28 natural images used in the psychophysical tests.

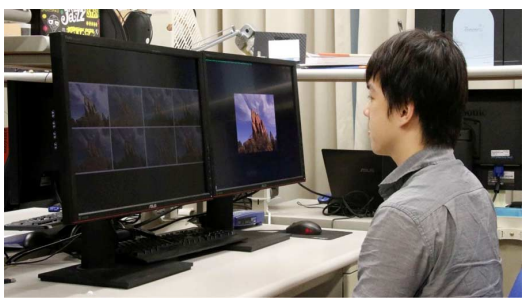

Fig. 14. Setup of the psychophysical tests. A low-backlight display and a full-backlight display are placed side by side in a well-illuminated lab.

duced by Gamma is so low that the images appear grayish although the lightness is effectively boosted. On the other hand, Pei over-boosts the dark regions (e.g. the parrot's body in the fifth column, the green pepper in the sixth column, and the dark hole of the center object in the seventh column). It can also be seen that Retinex produces undesirable ringing artifact due to low-pass filtering and that the resulting images appear grayish. Although Huang effectively enhances the details in the dark region, it sometimes fails to preserve the global contrast of the image. For example, the ceiling in the enhanced image in the second column appears almost as bright as the pillar on the right, but in fact it should be darker than the pillar.

VI. Psychophysical Tests

Two psychophysical tests were conducted to evaluate the performance of the proposed method. The 54 uniform color patches shown in Fig. 13(a) were used as test images in the first test, and the 28 natural images shown in Fig. 13(b) were used as test images in the second test. The uniform color patches were generated by the combination of three lightness levels, three chroma levels, and six hue values, whereas the set of natural images were selected such that it includes both indoor and outdoor scenes.

In both tests, two LCDs with the parameters specified in Table I were placed side by side in a well-illuminated lab. Two ViewSonic VG2427wm LCDs were used, one set to the full backlight level and the other to its lowest backlight level, as shown in Fig. 14. Each original image was displayed on the full-backlight LCD and the corresponding enhanced images produced by the methods described in Section V-B were displayed on the low-backlight LCD in random order. Twenty-six

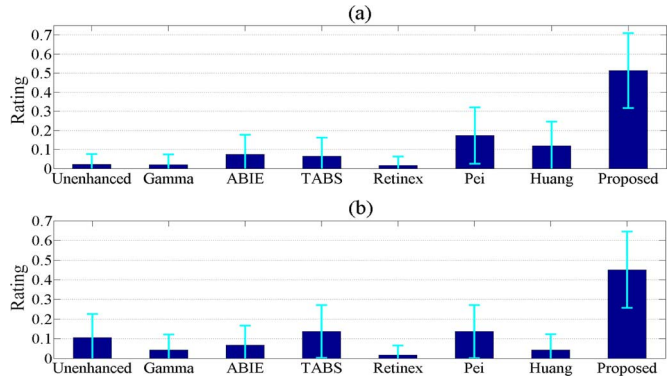

Fig. 15. Psychophysical test results for (a) color patches and (b) natural images. The horizontal axis represents different methods and the vertical axis is the probability that a method is rated best by subjects. The error bars represent the 95% confidence interval.

subjects with normal color vision were invited to participate in the tests and asked to choose from the enhanced images the one that appears closest to the original image. The viewing distance is approximately 50 cm, making the display extends approximately 63 degrees in the subject's field of view (FOV). Each color patch shown on the display extends approximately 8 degrees, and each natural image extends roughly 18 degrees in the subject's FOV. The images were shown with a black background to ensure that there is no brighter color stimulus within the central 63 degrees. The test room was set up such that no direct light source (e.g. lamp) or sun light appeared in the peripheral area beyond 63 degrees.

The results of the tests are shown in Fig. 15. For each method, we calculate the probability of being rated as the best by subjects. The error bars representing the 95% confidence interval are plotted to show the reliability of the results. We can see that the proposed method performs much better than the other methods.

VII. Discussion

In this section, we discuss the impact of the color appearance model on the proposed color image enhancement method, the significance of the post gamut mapping developed along with the proposed method, and some useful applications of the proposed method.

A. Selection of Color Appearance Model

CIECAM02 is adopted in this work to compute the relative perceptual attributes (i.e. lightness, chroma, and hue). Any other invertible color appearance models capable of predicting these attributes can be adopted in the algorithm. To investigate the impact of the color appearance models on the overall performance of color image enhancement, we substitute CIECAM02 with three other color appearance models: CIELAB [22], RLAB [23], and the Nayatani model [24], [25]. The Hunt model [26] is not considered because its inverse model, which cannot be expressed in an analytical form, is not as accurate as the above models [15].

The enhanced color patches and natural images are shown in Figs. 16 and 17, respectively. We can see that the CIELAB model does not preserve chroma and lightness very well and that

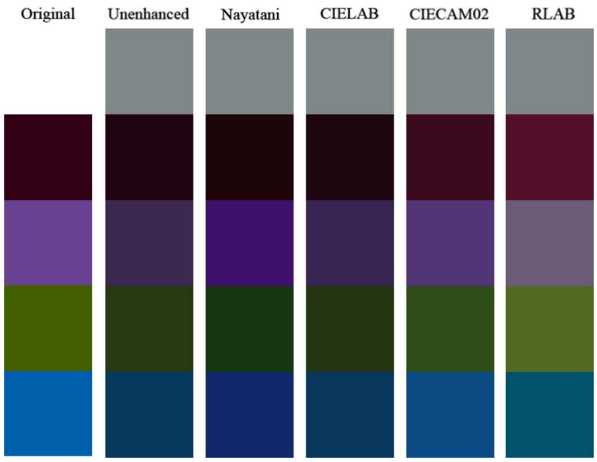

Fig. 16. Enhanced color patches generated by adopting various existing color appearance models in our algorithm. The name of the color appearance model used is shown at the top of each column.

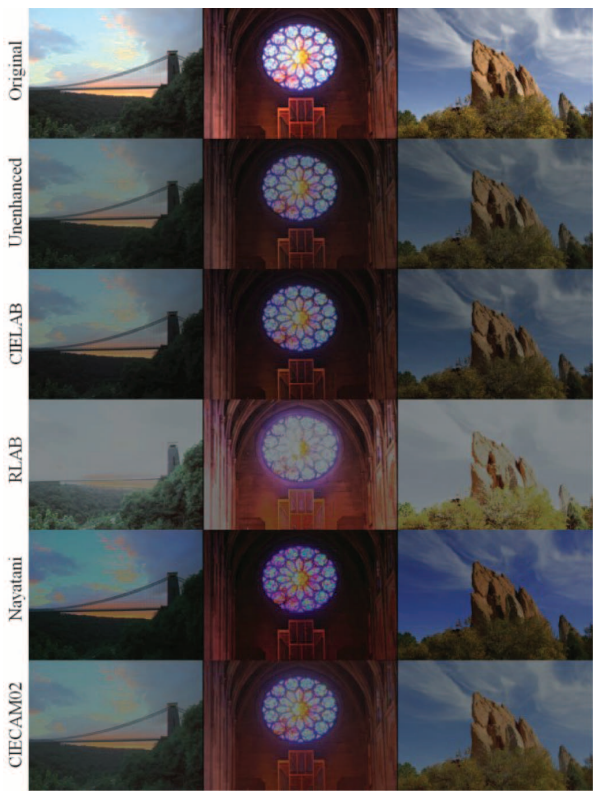

Fig. 17. Enhanced natural images generated by adopting various existing color appearance models in our algorithm. The name of the color appearance model is shown on the left of each row.

the output still appears dark and grayish. On the other hand, the RLAB model boosts the brightness effectively, but it produces overly exposed images and wipes out the details in bright regions as shown in the fourth row of Fig. 17. We can also see that the Nayatani model produces overly saturated images (see, for example, the sky region of the rock image in the third column of Fig. 17) because it is not originally designed for image reproduction applications [15].

It is clear that, among the four existing appearance models, CIECAM02 has the most robust and satisfactory performance.

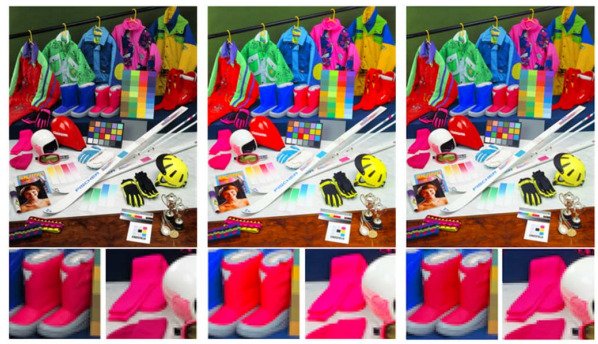

Fig. 18. Enhanced images generated by different gamut mapping strategies. (a) The original image. (b) The image generated by direct clipping. (c) The image generated by the proposed method. Selected close-ups of the enhanced images are shown in the second row.

TABLE II
COMPUTATION TIME OF THE PROPOSED METHOD

Input Image Size	1280x720	1920x1080
Number of Test Images	20	20
Average Computation Time (ms)	28.5	61.9
Standard Deviation (ms)	2.3	4.2

B. *Effect of Post Gamut Mapping*

Here we compare the images generated by two different post gamut mapping strategies: the proposed method and the method that directly clips the RGB value (10).

The results are shown in Fig. 18. We can see that although the image generated by direct clipping appears slightly brighter and more saturated than that produced by the proposed GMA, the image details in regions with highly saturated colors such as the texture on the boots and scarf are lost, as can be seen in the cropped close-ups. On the contrary, the proposed method effectively preserves the details in these regions without sacrificing the color appearance of less saturated regions such as the green background. The results show that the proposed method reproduces the color appearance of the original image and preserve the details of the image as well.

C. *Computation Time*

We test the speed of our method on HD (1280×720) images and full HD (1920×1080) images. Our algorithm is implemented in Matlab on a desktop computer running Windows 7 and with a 3.60 GHz Intel Core i3-4160 and a 6 GB memory. The average computation time is shown in Table II. We can see that our program can handle 16 full HD images per second and 35 HD images per second. This implies that our method is capable of enhancing video sequences in real time. In addition, the enhanced sequence is free of flicker due to the non-adaptive and spatially invariant nature of our method.

D. *Applications*

Our method was originally developed for thin film transistor LCD (TFT-LCD) with a backlight module to control the light intensity. But it can be applied to other panel displays, because all panel displays, including OLED and AMOLED, have a certain mechanism to control the light intensity and have the same

need for image color enhancement when the light intensity is low [43].

The application of the proposed method is not limited to the display of stored images or videos. It can be adopted in energy-aware video streaming services [16]–[19] where the computational load of color enhancement is placed on the server, instead of the clients, to achieve further energy saving. The server generates video at various energy-saving levels at the request of the clients.

In addition to the enhancement of backlight-scaled images, our method can also be applied to inverse tone mapping [44], [45] that expands the dynamic range of images for HDR displays and is essentially about the enhancement of image quality under a different display condition as well [46]. The only difference is the brightness of the anchor. In this application, our method can be applied to enhance the color appearance of images shown on multimedia devices with an HDR display to achieve better viewing experience.

VIII. Conclusion

In this paper, we have described a method for enhancing the color appearance of images illuminated with dim LCD backlight. Our method processes the luminance and chrominance components in an integral manner and hence avoids possible mismatches between luminance and chrominance adjustments. In addition, the method is simple enough for real-time enhancement of videos. Psychophysical tests show that the proposed method effectively improves the visual quality of backlight-scaled images and performs better than existing enhancement methods.

Acknowledgment

The authors would like to thank Prof. S.-L. Yeh for pointing out that the main idea described in this paper is called the anchoring property of HVS in vision science.

References

[1] Y. Nimmagadda, K. Kumar, and Y.-H. Lu, "Adaptation of multimedia presentations for different display sizes in the presence of preferences and temporal constraints," *IEEE Trans. Multimedia*, vol. 12, no. 7, pp. 650–664, Nov. 2010.

[2] C. Deng, W. Lin, and J. Cai, "Content-based image compression for arbitrary-resolution display devices," *IEEE Trans. Multimedia*, vol. 14, no. 4, pp. 1127–1139, Aug. 2012.

[3] A. Carroll and G. Heiser, "An analysis of power consumption in a smartphone," in *Proc. USENIX Annu. Technical Conf.*, Jun. 2010, pp. 21–34.

[4] Y. Wen, X. Zhu, J. J. P. C. Rodrigues, and C.-W. Chen, "Cloud mobile media: Reflections and outlook," *IEEE Trans. Multimedia*, vol. 16, no. 4, pp. 885–902, Jun. 2014.

[5] W. Yin, J. Luo, and C.-W. Chen, "Event-based semantic image adaptation for user-centric mobile display devices," *IEEE Trans. Multimedia*, vol. 13, no. 3, pp. 432–442, Jun. 2011.

[6] E. Reinhard *et al., High Dynamic Range Imaging: Acquisition, Display, Image-Based Lighting*, 2nd ed. San Mateo, CA, USA: Morgan Kaufmann, 2010.

[7] T.-H. Huang, C.-T. Kao, and H. H. Chen, "Quality enhancement of procam system by radiometric compensation," *IEEE Multimedia Signal Process. Workshop*, pp. 192–197, Sep. 2012.

[8] M. D. Grossberg, H. Peri, S. K. Nayar, and P. N. Belhumeur, "Making one object look like another: Controlling appearance using a projector-camera system," in *Proc. IEEE Comput. Soc. Conf. Comput. Vis. Pattern Recog.*, Jun. 2004, vol. 1, pp. I-452–I-459.

[9] N. Massouh, S. Colonnese, F. Cuomo, T. Okoya, and T. Pivsaev, "Experimental study on luminance preprocessing for energy-aware HTTP-based mobile video streaming," in *Proc. Eur. Workshop Vis. Inf. Process.*, Dec. 2014, pp. 1–6.

[10] G. Ghinea and J. P. Thomas, "Quality of perception: User quality of service in multimedia presentations," *IEEE Trans. Multimedia*, vol. 7, no. 4, pp. 786–789, Aug. 2005.

[11] A. Iranli, W. Lee, and M. Pedram, "HVS-aware dynamic backlight scaling in TFT-LCDs," *IEEE Trans. Very Large Scale Integr. Syst.*, vol. 14, no. 10, pp. 1103–1116, Oct. 2006.

[12] P.-S. Tsai, C.-K. Liang, T.-H. Huang, and H. H. Chen, "Image enhancement for backlight-scaled TFT-LCD displays," *IEEE Trans. Circuits Syst. Video Technol.*, vol. 19, no. 4, pp. 574–583, Apr. 2009.

[13] T.-H. Huang, K.-T. Shih, S.-L. Yeh, and H. H. Chen, "Enhancement of backlight-scaled images," *IEEE Trans. Image Process.*, vol. 22, no. 12, pp. 4587–4597, Dec. 2013.

[14] S.-C. Pei, C.-T. Shen, and T.-Y. Lee, "Visual enhancement using constrained L0 gradient image decomposition for low backlight displays," *IEEE Signal Process. Lett.*, vol. 19, no. 12, pp. 813–816, Dec. 2012.

[15] M. D. Fairchild, *Color Appearance Models*, 2nd ed. Chichester, U.K.: Wiley, 2005.

[16] T.-H. Lan and A. H. Tewfik, "A resource management strategy in wireless multimedia communications-total power saving in mobile terminals with a guaranteed QoS," *IEEE Trans. Multimedia*, vol. 5, no. 2, pp. 267–281, Jun. 2003.

[17] A. Lombardo, C. Panarello, and G. Schembra, "A model-assisted cross-layer design of an energy-efficient mobile video cloud," *IEEE Trans. Multimedia*, vol. 16, no. 8, pp. 2307–2322, Dec. 2014.

[18] Y. Wei, S. M. Bhandarkar, and S. Chandra, "A client-side statistical prediction scheme for energy aware multimedia data streaming," *IEEE Trans. Multimedia*, vol. 8, no. 4, pp. 866–874, Aug. 2006.

[19] R. Guruprasad and S. Dey, "Battery aware video delivery techniques using rate adaptation and base station reconfiguration," *IEEE Trans. Multimedia*, vol. 17, no. 9, pp. 1630–1645, Sep. 2015.

[20] K.-T. Shih and H. H. Chen, "Color enhancement based on the anchoring theory," in *Proc. IEEE Multimedia Signal Process. Workshop*, Sep.–Oct. 2013, pp. 153–158.

[21] T. Smith and J. Guild, "The C.I.E. colorimetric standards and their use," *Trans. Opt. Soc.*, vol. 33, no. 3, pp. 73–134, 1931.

[22] A. R. Robertson, "The CIE 1976 colour difference formulae," *Color Res. Appl.*, vol. 2, pp. 7–11, 1977.

[23] M. D. Fairchild and R. S. Berns, "Image color appearance specification through extension of CIELAB," *Color Res. Appl.*, vol. 18, pp. 178–190, Jun. 1993.

[24] Y. Nayatani *et al.*, "A nonlinear color appearance model using estévez-hunt-pointer primaries," *Color Res. Appl.*, vol. 12, pp. 231–242, Oct. 1987.

[25] Y. Nayatani *et al.*, "Color appearance model and chromatic adaptation transform," *Color Res. Appl.*, vol. 15, pp. 210–221, Aug. 1990.

[26] R. W. G. Hunt, "Revised colour appearance model for related and unrelated colours," *Color Res. Appl.*, vol. 16, pp. 146–165, Jun. 1991.

[27] N. Moroney *et al.*, "The CIECAM02 color appearance model," in *Proc. IS&T/SID 10th Color Imaging Conf.*, Nov. 2002, pp. 23–27.

[28] J. Morovic, *Color Gamut Mapping*. Chichester, U.K.: Wiley, 2008.

[29] J. Morovic and M. R. Luo, "The fundamentals of gamut mapping: A survey," *J. Imaging Sci. Technol.*, vol. 45, no. 3, pp. 283–290, 2001.

[30] J. Morovic, P.-L. Sun, and P. Morovic, "The gamuts of input and output colour reproduction media," in *Proc. SPIE Electron. Imaging*, Jan. 2001, pp. 114–125.

[31] G. J. Braun and M. D. Fairchild, "Image lightness rescaling using sigmoidal contrast enhancement functions," *J. Electron. Imaging*, vol. 8, no. 4, pp. 380–393, Oct. 1999.

[32] H.-S. Chen and H. Kotera, "Three-dimensional gamut mapping method based on the concept of image-dependence," in *Proc. IS&T NIP16 Conf.*, Jan. 2000, no. 1, pp. 783–786.

[33] L. W. MacDonald, J. Morovic, and K. Xiao, "A topographic gamut compression algorithm," *J. Imaging Sci. Technol.*, vol. 46, no. 3, pp. 228–236, Jun. 2001.

[34] H. Zeng, "Spring-primary mapping: Combining primary adjustment and gamut mapping for pictorials and business graphics," in *Proc. IS&T/SID 14th Color Imaging Conf.*, Nov. 2006, pp. 240–245.

[35] S. I. Cho, S.-J. Kang, and Y. H. Kim, "Image quality-aware backlight dimming with color and detail enhancement techniques," *J. Display Technol.*, vol. 9, no. 2, pp. 112–121, Feb. 2013.

[36] H. Cho and O.-K. Kwon, "A backlight dimming algorithm for low power and high image quality LCD applications," *IEEE Trans. Consum. Electron.*, vol. 55, no. 2, pp. 839–844, May 2009.

[37] N. Tamura, N. Tsumura, and Y. Miyake, "Masking model for accurate colorimetric characterization of LCD," *J. Soc. Inf. Display*, vol. 11, no. 2, pp. 333–339, 2003.
[38] R. S. Berns, R. J. Motta, and M. E. Gorzynski, "CRT colorimety," *Color Res. Appl.*, vol. 18, pp. 299–314, Oct. 1993.
[39] Y. Kwak and L. W. MacDonald, "Accurate prediction of colours on liquid crystal displays," in *Proc. IS&T/SID 9th Color Imaging Conf.*, Nov. 2001, pp. 355–359.
[40] "Colour measurement and management in multimedia systems and equipment. Part 4: Equipment using liquid crystal display panels," Int. Electrotech. Commission, Geneva, Switzerland, Tech. Rep. IEC 61966-4, 2000.
[41] C. Li *et al.*, "The performance of CIECAM02," in *Proc. IS&T/SID 10th Color Imaging Conf.*, Nov. 2002, pp. 28–32.
[42] Z. Rahman, D. J. Jobson, and G. A. Woodell, "Retinex processing for automatic image enhancement," *J. Electron. Imaging*, vol. 13, no. 1, pp. 100–110, Jan. 2004.
[43] C.-H. Lin, C.-K. Kang, and P.-C. Hsiu, "Catch your attention: Quality-retaining power saving on mobile OLED displays," in *Proc. 51st ACM/EDAC/IEEE Design Automat. Conf.*, Jun. 2014, pp. 1–6.
[44] F. Banterle, P. Ledda, K. Debattista, and A. Chalmers, "Inverse tone mapping," in *Proc. GRAPHITE*, 2006, pp. 349–356.
[45] T.-H. Wang *et al.*, "Pseudo-multiple-exposure-based tone fusion with local region adjustment," *IEEE Trans. Multimedia*, vol. 17, no. 4, pp. 470–484, Apr. 2015.
[46] K.-T. Shih, H. H. Chen, and Y.-N. Liu, "Image processing system and method," U.S. patent pending.

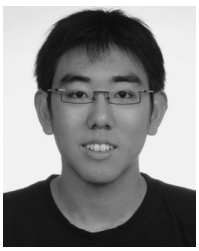

Kuang-Tsu Shih received the B.S. degree in electrical engineering from the National Taiwan University, Taipei, Taiwan, in 2009, and is currently working toward the Ph.D. degree in communication engineering at the National Taiwan University.

His current research interests include color image processing, color science, and computational photography.

Homer H. Chen (S'83–M'86–SM'01–F'03) received the Ph.D. degree in electrical and computer engineering from the University of Illinois at Urbana-Champaign, Urbana, IL, USA, in 1986.

Since August 2003, he has been with the College of Electrical Engineering and Computer Science, National Taiwan University, Taipei, Taiwan, where he is currently an Irving T. Ho Chair Professor. Prior to that, he held various research and development management and engineering positions with U.S. companies over a period of 17 years, including AT&T Bell Labs, Holmdel, NJ, USA; Rockwell Science Center, Thousand Oaks, CA, USA; iVast, Santa Clara, CA, USA; and Digital Island, Thousand Oaks, CA, USA. He was a U.S. delegate of the ISO and ITU standards committees and contributed to the development of many new interactive multimedia technologies that are now part of the MPEG-4 and JPEG-2000 standards. His current research interests include multimedia processing and communications.

Dr. Chen was an Associate Editor of the IEEE TRANSACTIONS ON CIRCUITS AND SYSTEMS FOR VIDEO TECHNOLOGY from 2004 to 2010, the IEEE TRANSACTIONS ON IMAGE PROCESSING from 1992 to 1994, and *Pattern Recognition* from 1989 to 1999. He served as a Guest Editor for the IEEE TRANSACTIONS ON CIRCUITS AND SYSTEMS FOR VIDEO TECHNOLOGY in 1999, the IEEE TRANSACTIONS ON MULTIMEDIA in 2011, the IEEE JOURNAL OF SELECTED TOPICS IN SIGNAL PROCESSING in 2014, and Springer *Multimedia Tools and Applications* in 2015. Currently he serves on the IEEE SPS Fourier Award Committee and Fellow Reference Committee.